

Performance enhancement of a terahertz patch antenna with metamaterials for 6G and biomedical applications

Siraj Younes¹, Kaoutar Saidi Alaoui², Jaouad Foshi¹

¹ERTTI Laboratory, Faculty of Science and Technology (FST) Errachidia, University of Moulay Ismail, Meknes, Morocco

²Higher School of Technology, Ibn Zohr University, Agadir, Morocco

Article Info

Article history:

Received Jun 1, 2024

Revised Oct 12, 2024

Accepted Oct 13, 2024

Keywords:

6G

Biomedical applications

HFSS

Metamaterials

Partial ground plane

Patch antenna

THz antenna

ABSTRACT

This paper introduces a novel approach for enhancing the performance of a terahertz (THz) patch antenna through the integration of metamaterials (MTM). The proposed design features a rectangular slotted patch antenna with a partial ground structure (DGS) that operates at 3.56 THz. The radiating element is situated on a substrate composed of silicon dioxide (SiO₂) with a dielectric of 4 and a thickness of 2 μm . The proposed MTM is a 6x5 elements with a FR4 substrate characterized by a dielectric of 4.2 and a thickness of 2 μm . The MTM is integrated beneath the antenna as a strategic technique to enhance its performance. The results confirm the significant impact of this integration. The MTM improves impedance matching and makes the antenna more directional. Consequently, the reflection coefficient is improved from -18.06 dB to -52.50 dB, the gain is increased from 1.72 dB to 3.49 dB, and the directivity also is enhanced from 3.69 dB to 5.10 dB. All results were obtained using HFSS software.

This is an open access article under the [CC BY-SA](https://creativecommons.org/licenses/by-sa/4.0/) license.



Corresponding Author:

Siraj Younes

ERTTI Laboratory, Faculty of Science and Technology (FST) Errachidia, University of Moulay Ismail
Meknes, Morocco

Email: sirajyounes95@gmail.com

1. INTRODUCTION

The exponential increase in data consumption and the pursuit of ultra-fast communication networks has led researchers to focus more research on the sixth generation (6G) of wireless communications. With anticipated features such as ultra-low latency, massive connectivity, and unprecedented data rates, 6G demands novel technological advancements. One critical component in achieving these goals is the development of efficient, high-frequency antennas. Terahertz (THz) patch antennas have emerged as promising candidates due to their ability to operate at the required high frequencies. Among these, the THz frequency range, typically defined as 0.1-10 THz in the electromagnetic spectrum, is a very good solution for many applications like the high-speed communication [1], biomedical [2], imaging [3], and sensing [4]. However, the effective utilization of the THz band presents substantial challenges and holds as a recent solution for various telecommunications applications, particularly in the design and performance optimization of patch antennas for biomedical applications.

Patch antennas are among the most popular types of antennas, with their low profile and ease of integration with other components like the wearable and portable devices, becomes a viable candidate for THz frequencies in the medical field. THz patch antennas has recently proposed as a good promise in the medical field due to their non-ionizing radiation characteristics, making them safe for medical use [5]. Moreover, this type of antenna provides high-resolution imaging of various components of the human body such as skin, tissues and teeth, aiding in early disease detection, such as cancer [6], [7], by identifying

abnormal tissue growth or composition changes. In other hands, These antennas facilitate non-invasive sensing of biological parameters, such as monitoring skin hydration [8], glucose levels [9], or assessing wound and burn conditions.

Patch antennas, with their many advantages at THz frequencies, is often hindered by some limitations such as low radiation, low efficiency, and high losses. To address these challenges, researchers have proposed various techniques, including slotting [10], [11], the utilization of partial ground planes [12], [13], the utilization of different substrate type [14] and superstrate meta surfaces [15]-[17]. Among all these strategies, the integration of metamaterials (MTM) techniques has emerged as a transformative approach and demonstrates satisfactory results. With their unique electromagnetic properties, MTM offer a potential solution to enhance the performance of THz antennas for 6G communication and biomedical applications.

MTM are artificially engineered structures designed to exhibit electromagnetic properties not found in natural materials [18]. Used recently in various domains, including the world of patch antennas. Integrating MTM into THz patch antennas helps achieve significant enhancements in key antenna parameters such as gain [19], bandwidth [20], and radiation efficiency. Significant contributions in the field of THz antennas and MTM have been made by various researchers. Smith *et al.* [21] explored the theoretical foundations and practical implementations of MTM, demonstrating their ability to manipulate electromagnetic waves in unconventional ways. Pendry *et al.* [22] introduced the concept of negative refractive index materials, paving the way for the development of MTM with unique properties. Shalaev [23] reviewed advancements in optical MTM, highlighting their potential in high-frequency applications, including antennas. Hossain *et al.* [24], a THz antenna designed for biomedical applications is introduced, specifically for detecting riboflavin with a resonance frequency of 3.731 THz and a return loss of -52.976 dB. Two THz patch antennas for cancer diagnosis applications are introduced in [25], [26], which operate within the THz frequency range and provide high-resolution imaging. The performance enhancement of patch antenna using reconfigurable intelligent surfaces (RIS) and MTM is proposed in [27], resulting in a gain increase of about 9 dB compared to conventional antennas. Komatineni *et al.* [28], a design using MTM with split ring resonators (SRRS) is presented, enhancing the patch antenna gain by 4.82 dBi. Furthermore, the bandwidth enhancement of patch antenna using MTM is presented in [29], the bandwidth was increased by 800 MHz by incorporating a complementary SRRS between the ground and the patch in the substrate.

Despite the advancements, several challenges remain in the development of THz patch antennas with MTM. High losses in MTM at THz frequencies limit the overall efficiency of the antennas. Achieving a broad operational bandwidth while maintaining high performance is challenging. The intricate structures of MTM pose significant fabrication challenges, especially at THz scales. Seamlessly integrating MTM-based THz antennas with existing communication systems requires further research.

This manuscript addresses the unresolved issues by proposing a novel design for a THz patch antenna integrated with advanced MTM. Unlike previous studies, our design focuses on loss minimization by employing novel MTM compositions and configurations, enhanced bandwidth, gain and radiation efficiency. We discuss the design principles of MTM-based THz antennas, highlighting the mechanisms through which MTM can improve antenna performance.

Our paper is structured as follows: the first section introduces the designs of the antenna and MTM, detailing their configurations and theoretical foundations. The second section conducts a comprehensive parametric study, examining the impact of various design parameters on the antenna performance. The third section provides an analysis of the obtained results. Finally, the paper concludes with a brief summary, some limitations and a discussion of future work. By addressing the critical challenges in THz antenna design and leveraging the unique properties of MTM, this research aims to contribute significantly to the development of high-performance antennas for the next generation of wireless communication and biomedical technologies.

2. METHOD

2.1. The patch antenna design

The dimensions of the antenna were calculated using following equations [10]:

$$W_p = \frac{c}{2f} \sqrt{\frac{2}{\epsilon_r + 1}} \quad (1)$$

where f is frequency, ϵ_r is dielectric of the substrate:

$$\epsilon_{ref} = \frac{\epsilon_r + 1}{2} + \frac{\epsilon_r - 1}{2} \left[1 + \frac{12h}{w} \right]^{\frac{1}{2}} \quad (2)$$

where ϵ_{ref} is the effective dielectric.

$$\Delta L = 0.412 h_s \frac{(\epsilon_{ref} + 0.3) \left(\frac{w}{h_s} + 0.264 \right)}{(\epsilon_{ref} - 0.258) \left(\frac{w}{h_s} + 0.8 \right)} \tag{3}$$

Where ΔL is the length extension:

$$L_p = L_{ef} - 2 \Delta L \tag{4}$$

$$L_{ef} = \frac{c}{2 f_r \sqrt{\epsilon_{ref}}} \tag{5}$$

where L_p is the patch length and L_{ef} is the effective length.

The proposed antenna is a slotted patch with partial ground plane, positioned over a silicon dioxide (SiO_2) substrate with a dielectric constant of 4 and a thickness of $2 \mu\text{m}$. The detailed architecture is presented in Figure 1, while the Table 1 provides the antenna dimension values. Operating at 3.56 THz, the antenna has dimensions of $W \times L$. In order to improve the antenna impedance matching, the radiating element features rectangular slots. Additionally, the size of the ground plane is reduced and the antenna is introduced with a partial ground with dimensions of $W \times L_g$. The design process, depicted in Figure 2, outlines the steps taken to achieve the final configuration. This design approach, including the specific substrate choice and the introduction of slots in the radiating patch, ensures optimal performance at our specified frequency.

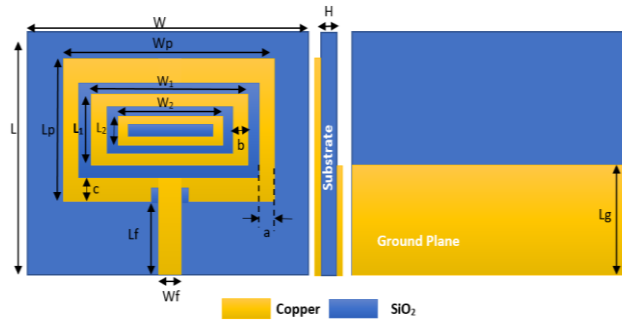


Figure 1. Structure of the proposed patch antenna

Table 1. Dimensions of the antenna

Variable	Value (μm)	Variable	Value (μm)
W	69	L2	11
L	54	Wf	4.8
L_p	35	Lf	15
W_p	46	a	3.5
W1	35	b	3
W2	25	c	5
L1	21	L_g	18.7
H	2		

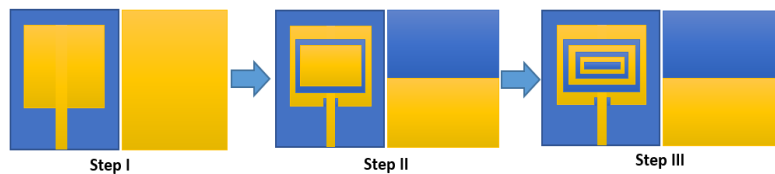


Figure 2. Design process of the proposed antenna

2.2. The metamaterial designs

The proposed MTM consists of a 6×5 array of elements, arranged on an FR4 substrate with a dielectric constant of 4.2, a loss tangent of 0.02, and a thickness of $2 \mu\text{m}$. Figure 3 illustrates the MTM details. The overall dimensions of the MTM are $W_{\text{MTM}} \times L_{\text{MTM}}$. Table 2 summarizes the MTM dimensions. The organization and structure of the split-ring resonator unit cells are depicted in Figure 3(a) and Figure 3(b)

respectively. Each unit cell within the array consists of periodic split-ring resonators spaced by $2 \mu\text{m}$ apart. The total size of each unit cell is $M_1 \times M_4$. In other hands, the FR4 substrate is chosen for its relatively low dielectric constant and low loss tangent, which helps minimize signal loss. The detailed simulation setup of the unit cell is depicted in Figure 3(c) illustrating the configuration used to analyze the electromagnetic behavior and performance of the MTM.

The performance of the MTM cell is evaluated using HFSS software to determine its electromagnetic characteristics. The S-parameters, phase, effective permittivity (ϵ_{eff}), and effective permeability (μ_{eff}) are calculated using MATLAB, with the simulation results presented in Figure 4. Utilizing the S-parameter method, which is widely adopted for retrieving material characteristics, the wave impedance and refractive index of the designed MTM cell can be determined. From these values, the equivalent electromagnetic permeability and permittivity can be calculated using a specific code on MATLAB. The S-parameter magnitudes show a resonance at 3.56 THz as illustrated in Figure 4(a), indicated by a dip in the reflection coefficient (S_{11}) and a peak in the transmission coefficient (S_{21}), suggesting optimal impedance matching and high transmission efficiency at this frequency. As presented in Figure 4(b), the phase changes in S_{11} and S_{21} around 3.5 THz further confirm the resonance. The effective medium parameters reveal a sharp peak in the real part of the effective permeability (μ_{eff}) at 3.5 THz, signifying a strong magnetic resonance. Meanwhile, the real part of the effective permittivity (ϵ_{eff}) remains positive over this frequency range, as illustrated in Figure 4(c), while the imaginary part exhibits a negative value, indicating stable dielectric characteristics. As shown in Figure 4(d), between 3.5 THz and 4.5 THz the equivalent permeability is negative, which efficiently suppresses surface waves.

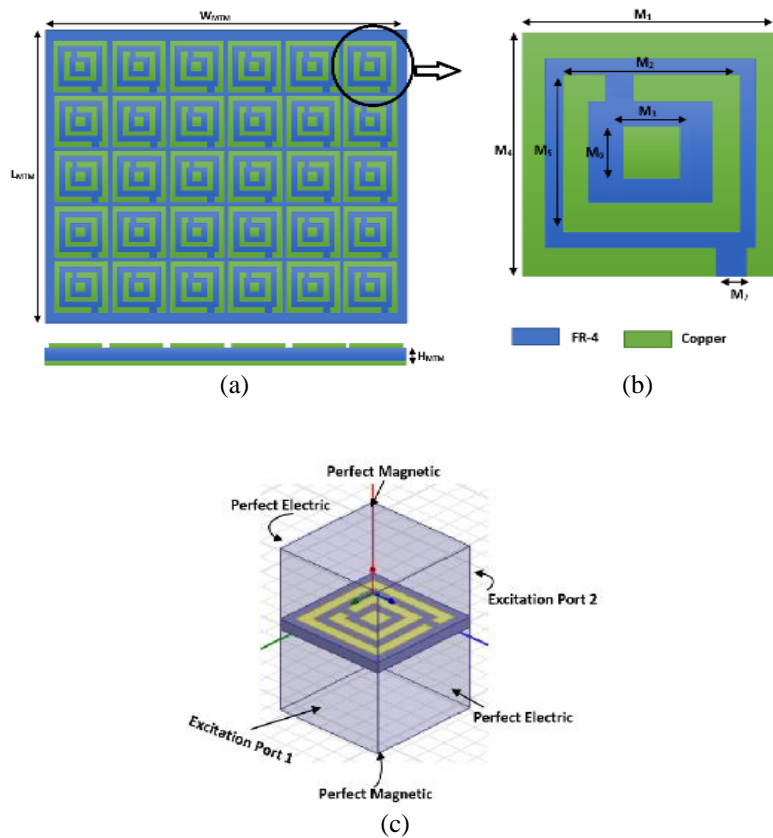


Figure 3. Design of the MTM; (a) organization of SRR, (b) unit cell, and (c) simulation setup

Table 2. Dimensions of the MTM

Variable	Value (μm)	Variable	Value (μm)
W_{MTM}	79	M3	2
L_{MTM}	64	M4	10
H_{MTM}	2	M5	6
M1	10	M6	2
M2	6	M7	1

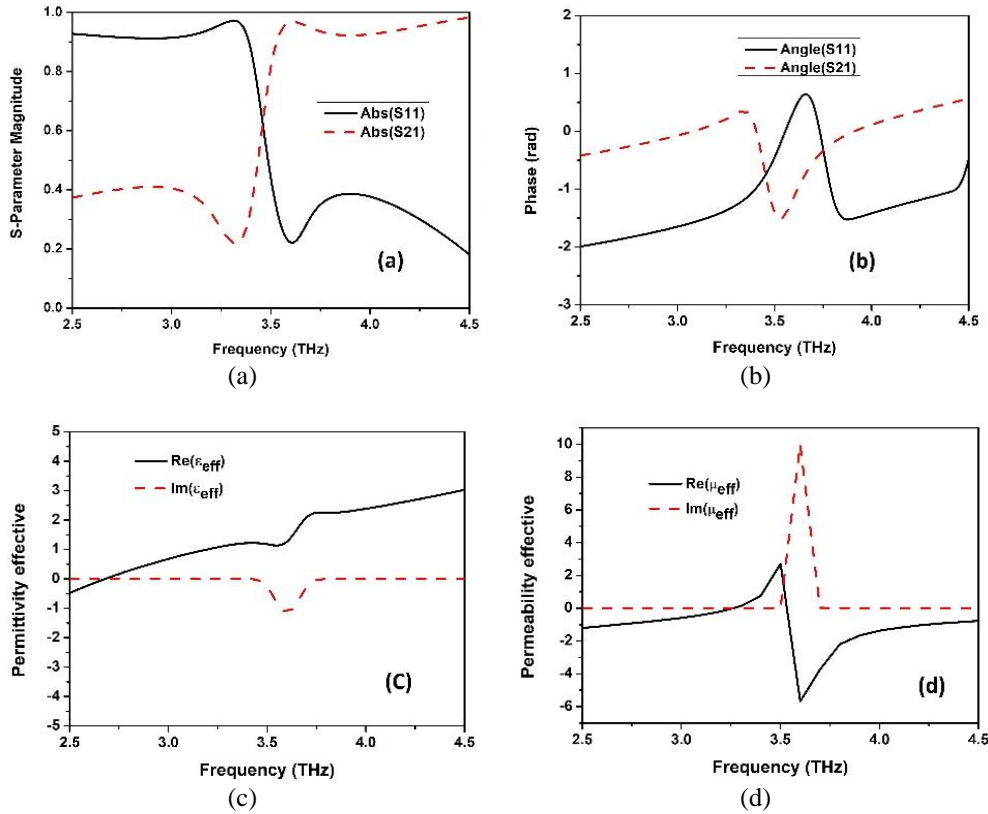


Figure 4. Unit cell parameters: (a) S-parameter magnitude, (b) phase, (c) permittivity, and (d) permeability

2.3. Position of the metamaterial and enhancement mechanism

The utilization of a partial ground plane in the antenna design helps to enhance the antenna impedance matching but it introduce some challenges related to antenna radiation characteristics, such as undesired back lobes and reduced Gain. To address this, the MTM is strategically positioned beneath the antenna at a precise spacing H_t of $13 \mu\text{m}$ as disputed in Figure 5. When MTM are positioned beneath an antenna, they enhance its performance through multiple mechanisms. Firstly, MTMs with negative permeability (in our case from 3.5 to 4.5 THz) create a specific reflection phase that causes destructive interference with backward-directed waves, thereby minimizing back radiation. Additionally, the MTM helps to suppress surface waves that typically propagate along the substrate and contribute to back radiation, which in turn improves efficiency. The MTM also function as artificial magnetic conductors (AMC), reflecting waves in phase with the incident waves to reinforce forward radiation and further reduce back radiation as presented in Figure 5.

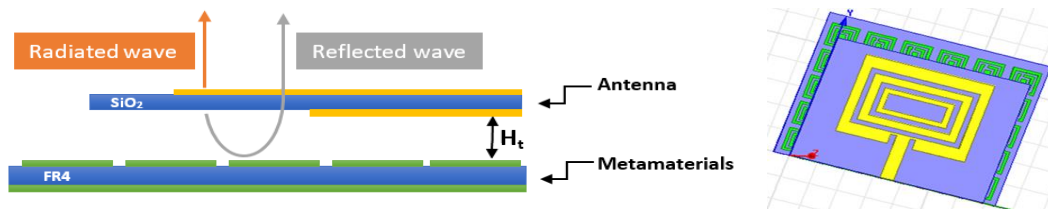


Figure 5. The position of the MTM and the antenna

3. PARAMETRIC STUDY

A parametric study was performed to evaluate the impact of certain key parameters into antenna performance, focusing on the reflection coefficient. This study involved systematically varying two critical design parameters, the dimensions of the partial ground plane and the spacing of the MTM.

3.1. Effect of the air Gap H_t

In order to evaluate the impact of the air gap between the antenna and the MTM, a parametric study was conducted, varying the H_t value within the range of 12 to 14 μm in 1 μm increments. The reflection coefficient was measured for each H_t value, as depicted in the Figure 6. The impact of the parameter is very clear, the best result is obtained with $H_t = 13 \mu\text{m}$ where the reflection coefficient was minimized and achieved a value of -52.50 dB, signifying optimal impedance matching and reduced reflection losses.

3.2. Effect of ground plane size L_g

Another parametric study was conducted to assess the influence of the antenna ground plane size. This study involved systematically varying L_g values from 16.7 to 19.7 μm in 1 μm increments. The reflection coefficient corresponding to each L_g value was analyzed and is depicted in the accompanying Figure 7. The impact of the parameter is very clear, the best result is obtained with $L_g = 18.7 \mu\text{m}$ with a S_{11} value of -52.50 dB. However, for the other L_g values, satisfactory results could not be attained, as the S_{11} parameter failed to surpass -20 dB. Indicating that the impedance matching was not achieved, and the antenna did not meet the desired criteria for optimal operation.

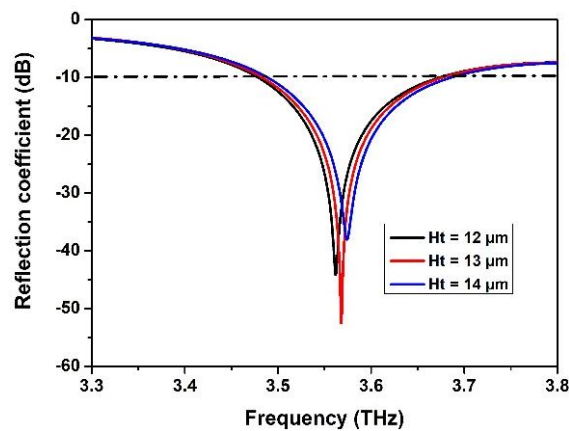


Figure 6. Return loss with different H_t values

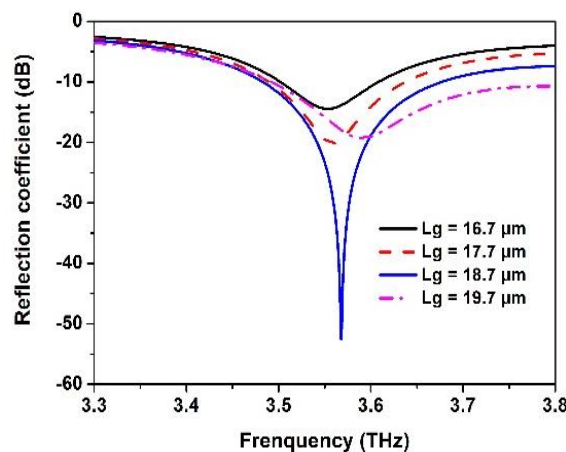


Figure 7. Return loss with different L_g values

4. RESULTS AND DISCUSSION

In this section, we analyzed the obtained results in detail and provided a comprehensive comparison between the antenna performance with and without the incorporation of the MTM. This comparison highlights the differences in key performance such as gain, bandwidth, reflection coefficient, and radiation patterns, demonstrating the impact of MTM on the antenna behavior. Additionally, we compared our findings with previous works to highlight the advancements achieved in this study.

4.1. Reflection coefficient and VSWR

The reflection coefficient (S_{11}) and voltage standing wave ratio (VSWR) are crucial indicators of antenna impedance matching and the level of reflected energy. The antenna operational range is typically determined by ensuring S_{11} is below -10 dB and VSWR is between 1 and 2. Figure 8 showcases the simulated results of the proposed antenna, where Figure 8(a) illustrates the return loss while Figure 8(b) presents the VSWR with and without MTM. The antenna alone achieved a S_{11} value of -18.06 dB due to the impedance mismatching, while the S_{11} enhanced to -52.50 dB when the MTM is integrated indicating the big influence of this integration on the antenna impedance matching. The antenna operates effectively within a frequency range of 3.47- 3.67 THz, boasting a bandwidth of 200 GHz. Furthermore, the VSWR also is enhanced and the antenna demonstrates exceptional value of 1.004, affirming excellent impedance matching. The MTM enhances the antenna reflection coefficient by improving impedance matching, leveraging its resonant properties, suppressing surface waves, and interacting with the near-field region of the antenna.

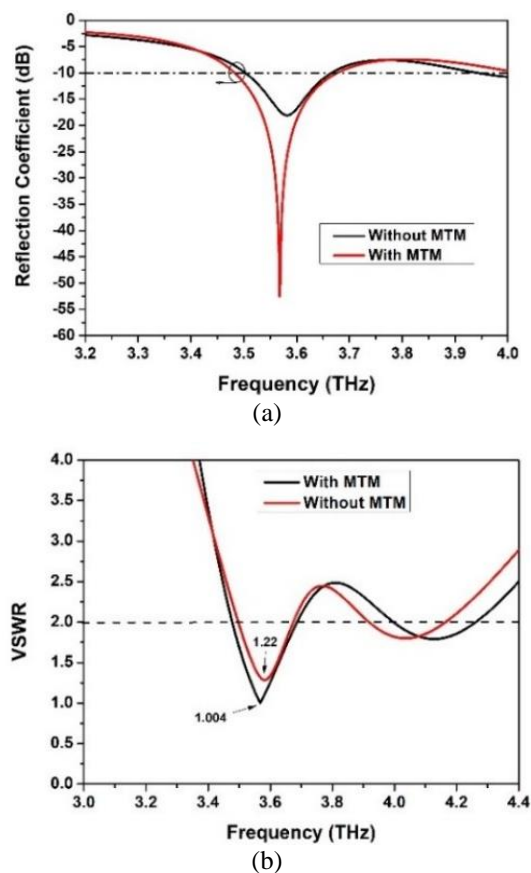


Figure 8. Simulated results of the proposed antenna (a) reflection coefficient and (b) VSWR of the proposed antenna with and without MTM

4.2. Gain

The radiation pattern serves as a crucial antenna characteristic, providing insight into its directional performance. In our study, the obtained radiations patterns are illustrated in Figure 9. The 2D radiation patterns of the proposed antenna with and without MTM are depicted in the Figure 9(a) and Figure 9(b) respectively. Meanwhile, Figure 9(c) and Figure 8(d) present the 3D radiation with and without MTM respectively. The gain value experienced a significant enhancement, increasing from 1.72 dB to 3.49 dB, marking a remarkable improvement of 102.92%. Indicating that more energy is effectively directed towards the desired direction. By concentrating electromagnetic fields and increasing the effective aperture, the MTM directs more energy in the desired direction. Additionally, it supports and manages surface waves, improving radiation efficiency. The MTM also shapes the antenna radiation pattern to focus energy more effectively and minimizes back radiation with its negative permeability characteristics, reducing energy loss in non-desired directions.

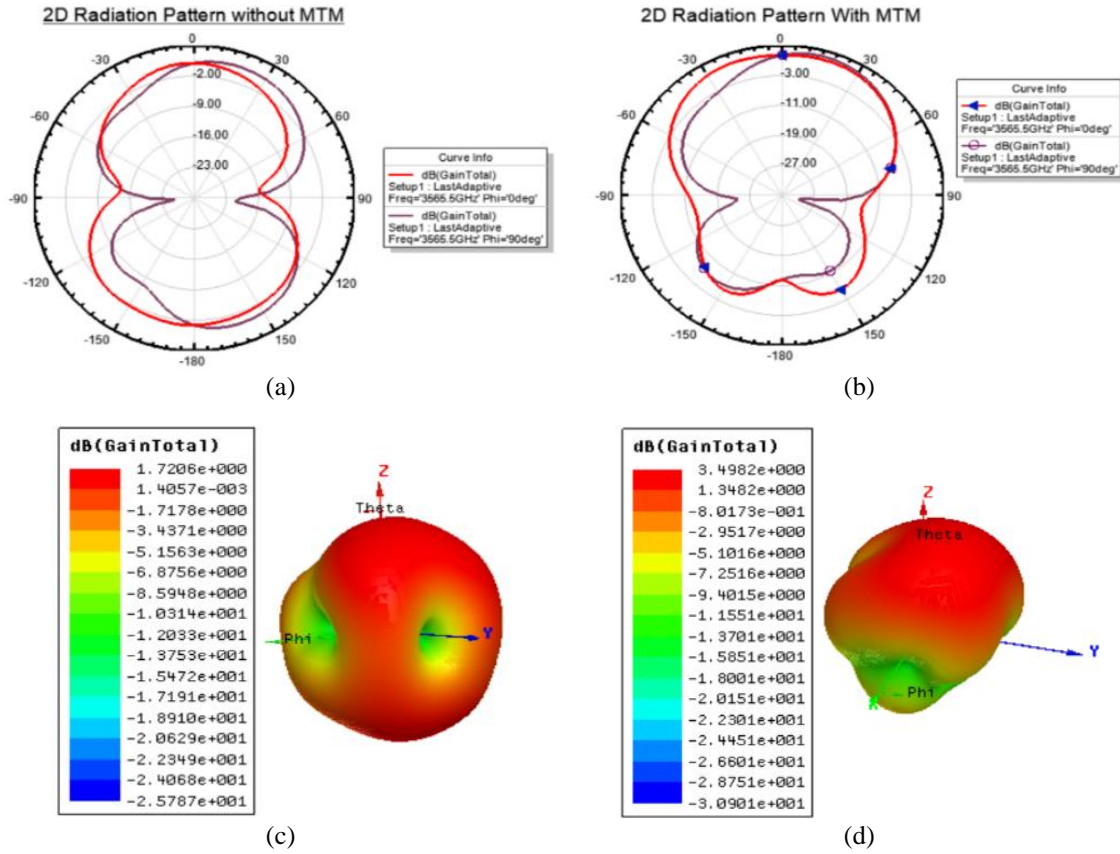


Figure 9. Radiation pattern: (a) 2D without MTM, (b) 2D with MTM, (c) 3D without MTM, and (d) 3D with MTM

4.3. Directivity

The directivity of an antenna represents its ability to concentrate radiated energy into a specific direction. The directivity of the proposed antenna was evaluated both with and without the integration of MTM as presented in Figure 10. Specifically, Figure 10(a) presents the obtained results without MTM, while Figure 10(b) displays the results with MTM. Initially, the proposed antenna exhibited a directivity of 3.69 dB. However, after incorporating MTM. The directivity increased to 5.10 dB marking a substantial improvement of 38.21%. This enhancement is primarily due to the MTM capacity to eliminate undesirable back radiation, thereby directing more energy forward. This focused radiation results in a more efficient antenna, making it highly beneficial for many biomedical applications requiring strong and clear signals.

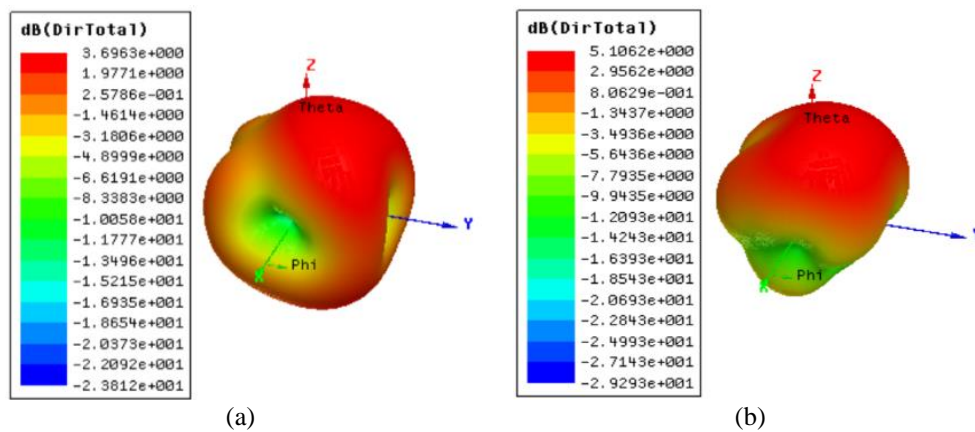


Figure 10. Directivity of our proposed antenna (a) without MTM and (b) with MTM

Table 3 summarizes the obtained results and provides a comprehensive comparison of the antenna performance with and without the integration of MTM in terms of several key parameters, including return loss, bandwidth, VSWR, gain, and directivity. By presenting these metrics side by side, the table provides a detailed and clear picture of how MTM integration leads to a more efficient and effective antenna design.

Table 3. Antenna performance comparison with and without MTM

	S_{11} (dB)	Bandwidth (GHz)	VSWR	Gain (dB)	Directivity (dB)
Without MTM	-18.06	150	1.22	1.72	3.69
With MTM	-52.50	200	1.004	3.49	5.10

Table 4 presents a detailed comparison of our proposed antenna with several antennas reported in the literature. This comparison includes critical parameters such as size, operating frequency, S_{11} , VSWR, and gain. Highlighting the superior performance of our proposed THz patch antenna. Our design, compared to [30], which has a much larger size of $1800 \times 1800 \mu\text{m}^2$ and an S_{11} of -43.60 dB, our antenna is significantly smaller while maintaining excellent impedance matching. Zubair *et al.* [31] operates at 3.65 THz with a size of $100 \times 100 \mu\text{m}^2$, an S_{11} of -29.00 dB, and a gain of 5.01 dB. While it shows a higher gain, our design achieves much better S_{11} , indicating superior impedance matching. In comparison to [32], which operates at 3.62 THz with a very compact size of $30 \times 20 \mu\text{m}^2$ and an S_{11} of -12.25 dB, our antenna offers significantly better impedance matching and a more favorable VSWR (1.004 vs. 1.646). Khaalel *et al.* [33] has an S_{11} of -63.69 dB, but its gain is only 1.37 dB, much lower than the 3.49 dB achieved by our design.

Table 4. Comparison of our proposed work with previous works

Ref.	Size (μm^2)	Frequency (THz)	S_{11} (dB)	VSWR	Gain (dB)
[30]	$1,800 \times 1,800$	3.5	-43.60	1.013	-
[31]	100×100	3.65	-29.00	-	5.01
[32]	30×20	3.62	-12.25	1.646	-
[33]	120×95	3.5	-63.69	1.003	1.37
[This work]	69×54	3.56	-52.50	1.004	3.49

5. CONCLUSION




In this work, we have demonstrated the significant performance enhancements of a THz patch antenna through the strategic integration of MTM. By incorporating a 6×5 element MTM structure beneath a rectangular slotted patch antenna with a partial ground structure (DGS), operating at 3.56 THz, we achieved notable improvements in key antenna parameters. The MTM integration markedly improves impedance matching, resulting in a substantial reduction of the reflection coefficient from -18.06 dB to -52.50 dB. Additionally, the antenna gain increased from 1.72 dB to 3.49 dB, and its directivity enhanced from 3.69 dB to 5.10 dB. These advancements validate the effectiveness of integrating MTM in addressing the intrinsic limitations of THz patch antennas, especially in improving radiation pattern efficiency, gain, and bandwidth. In the biomedical field, such improvements have the potential to transform imaging and sensing technologies, enabling more precise and non-invasive diagnostic techniques that could significantly aid in early disease detection and monitoring. Overall, this research establishes a foundation for future technological progress and provides practical benefits that could enhance both 6G communication systems and medical diagnostics. However, it is important also to acknowledge the limitations in the development of THz MTM and patch antenna. Fabrication precision at THz frequencies is challenging due to the small wavelength, requiring advanced techniques like electron-beam lithography, which are expensive and time consuming. Additionally, the materials used at these frequencies often exhibit higher losses, impacting overall efficiency. These limitations highlight the need for ongoing research and innovation to fully realize the potential of THz MTM and antennas. For further experiments with the proposed antenna, specific absorption rate (SAR) calculations can be performed to evaluate its safety and effectiveness, particularly in biomedical applications.

REFERENCES




- [1] H. Vettikalladi, W. T. Sethi, A. F. Bin Abas, W. Ko, M. A. Alkanhal, and M. Himdi, "Sub-THz antenna for high-speed wireless communication systems," *International Journal of Antennas and Propagation*, vol. 2019, pp. 1–9, Mar. 2019, doi: 10.1155/2019/9573647.
- [2] N. Goswami and M. A. Rahman, "A 9.73 GHz wide-band off-body patch antenna for biomedical applications," *Indonesian Journal of Electrical Engineering and Computer Science (IJECS)*, vol. 33, no. 1, pp. 151–158, Jan. 2024, doi: 10.11591/ijeecs.v33.i1.pp151-158.
- [3] A. S. Dhillon, D. Mittal, and E. Sidhu, "THz rectangular microstrip patch antenna employing polyimide substrate for video rate imaging and homeland defence applications," *Optik*, vol. 144, pp. 634–641, Sep. 2017, doi: 10.1016/j.ijleo.2017.07.018.

- [4] G. Saxena *et al.*, “CSRR loaded multiband THz MIMO antenna for nano-communications and bio-sensing applications,” *Nano Communication Networks*, vol. 38, p. 100481, Dec. 2023, doi: 10.1016/j.nancom.2023.100481.
- [5] Fajr, A. Rajawat, and S. H. Gupta, “Design and optimization of THz antenna for onbody WBAN applications,” *Optik*, vol. 223, p. 165563, Dec. 2020, doi: 10.1016/j.jllo.2020.165563.
- [6] M. Kumar, S. Goel, A. Rajawat, and S. H. Gupta, “Design of optical antenna operating at Terahertz frequency for In-Vivo cancer detection,” *Optik*, vol. 216, p. 164910, Aug. 2020, doi: 10.1016/j.jllo.2020.164910.
- [7] S. P. Khanjari and F. B. Zarrabi, “Reconfigurable Vivaldi THz antenna based on graphene load as hyperbolic metamaterial for skin cancer spectroscopy,” *Optics Communications*, vol. 480, p. 126482, Feb. 2021, doi: 10.1016/j.optcom.2020.126482.
- [8] A. I. Hernandez-Serrano *et al.*, “Terahertz probe for real time in vivo skin hydration evaluation,” *Advanced Photonics Nexus*, vol. 3, no. 01, Feb. 2024, doi: 10.1117/1.AP.N.3.1.016012.
- [9] J. Yang *et al.*, “A terahertz metamaterial sensor used for distinguishing glucose concentration,” *Results in Physics*, vol. 26, p. 104332, Jul. 2021, doi: 10.1016/j.rinp.2021.104332.
- [10] Y. Siraj, K. S. Alaoui, and J. Foshi, “Study and design of a patch antenna for biomedical applications,” *ITM Web of Conferences*, vol. 52, p. 03003, May 2023, doi: 10.1051/itmconf/20235203003.
- [11] M. F. Ahmed, A. Z. M. T. Islam, and M. H. Kabir, “Rectangular microstrip antenna design with multi-slotted patch and partial grounding for performance enhancement,” *International Journal of Electrical and Computer Engineering (IJECE)*, vol. 12, no. 4, pp. 3859–3868, Aug. 2022, doi: 10.11591/ijece.v12i4.pp3859-3868.
- [12] S. Younes and F. Jaouad, “Wearable patch antenna with rectangular slots and defected ground for biomedical applications,” in *2023 IEEE International Conference on Contemporary Computing and Communications (InC4)*, Apr. 2023, pp. 1–6, doi: 10.1109/InC457730.2023.10263109.
- [13] M. L. El Issawi, D. B. O. Konditi, and A. D. Usman, “Design of an enhanced dual-band microstrip patch antenna with defected ground structures for WLAN and WiMax,” *Indonesian Journal of Electrical Engineering and Computer Science (IJECS)*, vol. 35, no. 1, pp. 165–174, Jul. 2024, doi: 10.11591/ijeecs.v35.i1.pp165-174.
- [14] A. A. Abubakar and Z. Yunusa, “Comparative analysis of microstrip patch antenna on different substrate material using slit technique for x-band application,” 2021, [Online]. Available: <https://www.researchgate.net/publication/351870270>.
- [15] A. K. Jassim, M. J. Farhan, and F. N. H. Al-Nuaimy, “Enhancement of gain using a multilayer superstrate metasurface cell array with a microstrip patch antenna,” *Indonesian Journal of Electrical Engineering and Computer Science (IJECS)*, vol. 24, no. 3, pp. 1564–1570, Dec. 2021, doi: 10.11591/ijeecs.v24.i3.pp1564-1570.
- [16] V. S. Rao, K. V. V. S. Redd, and A. M. Prasad, “Bandwidth enhancement of metamaterial loaded microstrip antenna using double layered substrate,” *Indonesian Journal of Electrical Engineering and Computer Science (IJECS)*, vol. 5, no. 3, pp. 661–665, Mar. 2017, doi: 10.11591/ijeecs.v5.i3.pp661-665.
- [17] S. Said, S. El Mattar, A. Faize, A. Es-Salhi, B. Elhadi, and A. Baghdad, “Patch antenna design based on 1D-EBG structures for high gain applications,” *Telkomnika (Telecommunication Computing Electronics and Control)*, vol. 21, no. 6, pp. 1178–1184, Dec. 2023, doi: 10.12928/TELKOMNIKA.v21i6.24945.
- [18] N. Kim, Y.-J. Yoon, and J. B. Allen, “Generalized metamaterials: definitions and taxonomy,” *The Journal of the Acoustical Society of America*, vol. 139, no. 6, pp. 3412–3418, Jun. 2016, doi: 10.1121/1.4950726.
- [19] G. H. Khouser, Y. K. Choukiker, and A. Bhowmick, “Gain enhancement in microstrip patch antenna with high negative refractive index 3D-metamaterial inspired superstrate for wireless applications,” *IEEE Access*, vol. 12, pp. 7372–7381, 2024, doi: 10.1109/ACCESS.2024.3352118.
- [20] I. Sansa, A. Nasri, and H. Zairi, “Bandwidth enhancement of an antenna based metamaterial using characteristic mode analysis for microwave applications,” *Journal of Engineering Science and Technology*, vol. 18, no. 1, pp. 636–652, 2023.
- [21] D. R. Smith, J. B. Pendry, and M. C. K. Wiltshire, “Metamaterials and negative refractive index,” *Science*, vol. 305, no. 5685, pp. 788–792, Aug. 2004, doi: 10.1126/science.1096796.
- [22] J. B. Pendry, A. J. Holden, D. J. Robbins, and W. J. Stewart, “Magnetism from conductors and enhanced nonlinear phenomena,” *IEEE Transactions on Microwave Theory and Techniques*, vol. 47, no. 11, pp. 2075–2084, 1999, doi: 10.1109/22.798002.
- [23] V. M. Shalaev, “Optical negative-index metamaterials,” *Nature Photonics*, vol. 1, no. 1, pp. 41–48, Jan. 2007, doi: 10.1038/nphoton.2006.49.
- [24] T. Hossain, M. Parvez, A. Z. Md.Imran, M. J. Uddin, A. Gafur, and S. Z. Rashid, “TeraHertz antenna for biomedical application,” in *2022 International Conference on Innovations in Science, Engineering and Technology (ICISSET)*, Feb. 2022, pp. 42–45, doi: 10.1109/ICISSET54810.2022.9775884.
- [25] S. H. Gupta, S. Goel, M. Kumar, A. Rajawat, and B. Singh, “Design of terahertz antenna to detect lung cancer and classify its stages using machine learning,” *Optik*, vol. 249, p. 168271, Jan. 2022, doi: 10.1016/j.jllo.2021.168271.
- [26] D. E. R. Kanmani, W. S. Edwin, P. Ponnusamy, “Terahertz imaging patch antenna for cancer diagnosis applications,” *International Journal of Engineering and Advanced Technology*, vol. 9, no. 3, pp. 3258–3261, Feb. 2020, doi: 10.35940/ijeat.C4735.029320.
- [27] S. K. Budarapu, M. S. Sunder, and B. Ramakrishna, “Performance enhancement of patch antenna using RIS and metamaterial superstrate for wireless applications,” *Progress In Electromagnetics Research C*, vol. 130, pp. 95–105, 2023, doi: 10.2528/PIERC22112603.
- [28] R. Komatineni, C. S. Hruday, V. S. Vutukuru, and V. Dasari, “Millimeter wave MPA using metamaterial-substrate antenna array for gain enhancement,” Nov. 13, 2023, doi: 10.36227/techrxiv.24516250.v1.
- [29] H. A. Al Issa, Y. S. H. Khraisat, and F. A. S. Alghazo, “Bandwidth enhancement of microstrip patch antenna by using metamaterial,” *International Journal of Interactive Mobile Technologies (iJIM)*, vol. 14, no. 01, p. 169, Jan. 2020, doi: 10.3991/ijim.v14i01.10618.
- [30] V. Koushick, C. Divya, M. Vinoth, E. A. M. Ali, and M. Sugadev, “THz microstrip antenna for terabit wireless local area networks,” *The Applied Computational Electromagnetics Society Journal (ACES)*, vol. 38, no. 7, pp. 522–531, Dec. 2023, doi: 10.13052/2023.ACES.J.380708.
- [31] M. Zubair, A. Jabbar, M. O. Akinsolu, M. A. Imran, B. Liu, and Q. H. Abbasi, “Design of truncated microstrip square patch antenna for terahertz communication,” in *2022 IEEE International Symposium on Antennas and Propagation and USNC-URSI Radio Science Meeting (AP-S/URSI)*, Jul. 2022, pp. 1558–1559, doi: 10.1109/AP-S/USNC-URSI47032.2022.9886809.
- [32] Z. Mezache, “Analysis of multiband graphene-based terahertz square-ring fractal antenna,” *Ukrainian Journal of Physical Optics*, vol. 21, no. 2, pp. 93–102, 2020, doi: 10.3116/16091833/21/2/93/2020.
- [33] S. A. Khaleel, E. K. I. Hamad, and M. B. Saleh, “High-performance tri-band graphene plasmonic microstrip patch antenna using superstrate double-face metamaterial for THz communications,” *Journal of Electrical Engineering*, vol. 73, no. 4, pp. 226–236, Aug. 2022, doi: 10.2478/jee-2022-0031.




BIOGRAPHIES OF AUTHORS

Siraj Younes    received his master's degree in industrial computer engineering and instrumentation from the Faculty of Science and Technology Errachidia (FSTE), Moulay Ismail University, Morocco, in 2020. Presently, he is pursuing a Ph.D. at FSTE in Errachidia, Moulay Ismail University, Meknes, starting in 2022. His research focuses on the design and optimization of patch antennas for biomedical applications. He can be contacted at email: y.siraj@edu.umi.ac.ma.



Kaoutar Saidi Alaoui    assistant professor of Higher Education in Telecommunications and electronics at the Dakhla Higher School of Technology, Ibn Zohr University, Agadir Morocco since 2021, she obtained his National Doctorate in 2020 from the Faculty of Science and Technology in Errachidia at Moulay Ismail University in Meknes, Morocco. Currently, she's the coordinator of the electrical engineering branch at the Dakhla Higher School of Technology. Her research interests encompass Optical fiber, OCDMA and patch antennas for biomedical applications. She can be contacted at email: k.alaouisaidi@uiz.ac.ma.



Jaouad Foshi    professor of Higher Education in Telecommunications at the Faculty of Science and Technology in Errachidia Morocco since 2008, he obtained his National Doctorate in 2001 from the Faculty of Sciences at Moulay Ismail University in Meknes, Morocco. Currently, he serves as the dean of FSTE. His research interests encompass the investigation of patch antennas in various applications. He can be contacted at email: j.foshi@fste.umi.ac.ma.